

Contents lists available at ScienceDirect

# Journal of Terramechanics

journal homepage: www.elsevier.com/locate/jterra



# Review of modeling methods of compressed snow-tire interaction



Yogesh Surkutwar a,\*, Corina Sandu b, Costin Untaroiu a

- <sup>a</sup> Department of Biomedical Engineering & Mechanics, Virginia Tech, Blacksburg, VA, United States
- <sup>b</sup> Department of Mechanical Engineering, Virginia Tech, Blacksburg, VA, United States

#### ARTICLE INFO

# Article history: Received 4 July 2022 Revised 1 October 2022 Accepted 24 October 2022 Available online 10 November 2022

Keywords:
Compacted snow
Snow material models
Snow material properties
Finite Element Method (FEM)
Arbitrary Lagrangian Eulerian (ALE) method
Smoothed Particle Hydrodynamics (SPH)
method
Discrete Element Method (DEM)

# ABSTRACT

Snow traction is a key performance characteristic for tire design. Designing snow tires requires extensive testing on snow-covered proving grounds. Thus, numerical simulation could be a more efficient and less costly method of improving tire designs. Various numerical approaches, such as analytical methods, grid-based methods, and particle-based methods were employed for compacted snow modeling in literature. Analytical models of compacted snow were developed based on various assumptions about snow mechanics and tire-snow interaction. With increasing the computational power, grid-based methods (especially Arbitrary Lagrangian Eulerian method) showed to provide effective modeling of complex tire-snow interaction behavior. However, these approaches showed some limitations in modelling large and discontinuous deformation problems associated with tire-snow interaction. Therefore, recently, the use of particle-based methods, which overcome these limitations, has recently sparked interest in tire-snow modeling. The numerical studies related to the modeling tire-snow interaction are briefly reviewed in this paper. Furthermore, various constitutive snow material models and different failure theories used in literature, which are essential for numerical tire-compacted snow simulations, are also reviewed. Overall, this review paper could be useful for researchers interested in modeling the tire – snow interactions and even tire-deformable soil interaction.

 $\ensuremath{\texttt{©}}$  2022 ISTVS. Published by Elsevier Ltd. All rights reserved.

## **Contents**

1.	Introduction	28
2.	Snow properties and material models	29
	2.1. Snow properties	29
	2.1.1. Snow density and mechanical properties	29
	2.1.2. Young's modulus of snow	29
	2.2. Snow material models	30
	2.3. Snow failure models	31
	2.3.1. Mohr-Coulomb failure criterion.	31
	2.3.2. Drucker-Prager failure criterion.	32
	2.3.3. Modified-Drucker Prager with cap failure criterion	32
	2.3.4. Cam-clay and modified cam-clay failure criterion	33
3.	Modeling of tire-snow interaction	35
	3.1. Analytical/semi-analytical methods	35
	3.2. Finite element methods	36
	3.3. Particle based methods	37
	3.3.1. Smoothed particle Hydrodynamics (SPH) method	37
	3.3.2. Discrete element method (DEM)	37
4.	Conclusion	38
	Declaration of Competing Interest	38
	Acknowledgments	38
	References	39

E-mail addresses: yogeshvs@vt.edu, yogeshvs@vt.edu (Y. Surkutwar).

<sup>\*</sup> Corresponding author.

Nome	nclature		
P	Pressure	$k_c$	Cohesion constant
$k_{\phi}$	Friction angle constant	b	Width of contact patch
Z	Sinkage	j	Shear Displacement
$f_{rr}$	Rolling resistance	n	Number of blows
W	Weight of hammer	h	Height of hammer drop
$S_n$	Sinkage after 'n' blows	Q	Weight of assembly
ψ	Strain rate	τ	Shear stress
C	Material cohesion	ф	Material angle of friction
Q	Deviatoric Stress	Ē	Young's Modulus
$\rho$	Density	$\sigma_{\rm c}$	Unconfined compressive strength
$ au_{oct}$	octahedral shear stress	$\sigma_{oct}$	octahedral normal stress
R	Cap eccentricity parameter	G	Shear modulus
λ	Consolidation index	k	swelling recompression index
N	Specific volume at unit hydrostatic pressure	M	Slope of critical state line
$q_0$	Pre-consolidation pressure	μ	coefficient of internal friction
$J_2$	Second invariant of the stress deviator tensor	$I_1^{\prime}$	The first invariant of the stress tensor
$F_s$	Share failure surface	$F_c$	Compression cap
p	Hydrostatic pressure stress	q	Deviatoric stress measure, or Von Mises equivalent
$oldsymbol{p}'$	Effective mean stress		stress
ν	Specific volume	$q^{'}$	Deviatoric (shear stress)
$\lambda^{'}$	Slope of the normal compression	κ	Slope of swelling line
$F_S$	Shear force of snow in void	Γ	specific volume of the CSL
$F_B$	Braking force	$F_{\mu}$	Frictional force between tire and snow
$\sigma_n$	Normal stress	$\dot{F_{D}}$	digging force
$F_x$	drawbar pull	$F_{\tau x}$	Traction Force

#### 1. Introduction

Snow traction is an important key performance parameter for tires. However, the highly nonlinear properties of compacted snow. flexible tires, and the contact mechanics at the tire-snow interface provides significant challenges in predicting snow traction. There are many factors that influences the tire-snow interaction, including interfacial slips, normal load on the wheel, friction coefficient at the interface, and snow depth. Accurate numerical prediction of snow traction is challenging mainly due to the lack of reliable material models of compressed snow and accurate modelling of tire-snow interaction (Lee, 2011a, Lee 2013). Snow shows highly complex characteristics under normal conditions, exhibiting nonlinear viscoelasticity and undergoing large strains, both volumetric and deviatoric (Mellor 1975, Shenvi et al., 2022). As a result, formulating rigorous constitutive equations and failure criteria in the context of continuum mechanics, which are necessary for numerical simulations, has proven to be challenging. Several researchers suggested the need for the development of improved material models as present state-of-the-art snow material models defined in FEA software perform poorly (Hambleton and Drescher 2008, Terziyski 2010).

There are several methods in the literature for modeling snow-tire interaction behavior, such as analytical and semi-analytical methods (Nakajima 2003), finite element methods (Mundl et al., 1997, Seta et al., 2010, Terziyski 2010) and the recently developed particle-based methods (Xu et al., 2020, Bui and Nguyen 2021). Each method has its own advantages and disadvantages, which are thoroughly discussed in this study. In analytical and semi-analytical methods, mathematical relationships are used to calculate the forces and moments at the tire-snow interaction (Nakajima 2003, Lee and Liu 2006). Then, snow traction are predicted using braking force due to snow compression, shear force of snow in the void, frictional force, and digging force. In finite element methods (FEM), the snow is modeled using various material models (e.g., Mohr-Coulomb yield model, a modified Drucker-Pra-

ger with a cap, and Cam-Clay yield model, etc.) which are suitable for capturing the highly compressible behavior of snow (Meschke et al., 1996, Shoop 2001, Seta et al., 2003). Before to be used in the numerical simulations of complex tire-snow interactions, these material models should be validated/calibrated against simple compression/shear tests (e.g. compression and shear tests). The particle-based methods are appropriate when dealing with free surface flow and large deformation and have recently attracted attention in snow modeling. These methods are divided into two types: continuum methods and discrete methods (Karajan et al., 2014). The continuum methods requires no background mesh for numerical integration of governing equations, avoiding some of the drawbacks of computational mesh when dealing with large deformation or even complete detachment. The Smoothed Particle Hydrodynamics (SPH) method (Bui et al., 2007, El-Sayegh and El-Gindy, 2018, Bui and Nguyen, 2021) is the most commonly used continuum particle-based method for tire-snow interaction studies. In a discrete particle-based method, particles interact with other particles using Newton's equation of motion and a contact law to determine the inter-particle contact forces. The Discrete Element Method (DEM) (Johnson and Hopkins 2005, Theile et al., 2020, Xu et al., 2020) is one of the most widely used discrete approaches in tire-snow interaction modeling. Hence, SPH and DEM approaches appears to be a promising alternative for modeling snow behavior among the particle-based methods.

The aim of this literature review is to acquire a better understanding of the present state of knowledge about various modeling methodologies for compacted snow-tire interaction studies. The study starts with a brief review of material properties of snow, constitutive material model proposed to model snow and corresponding failure theories. Then, the numerical methods proposed in literature to investigate tire-snow interaction are reviewed with a special interest in snow modelling. Finally, some conclusions are provided which could be the basis for future improvements of snow modelling for better numerical prediction of snow traction.

## 2. Snow properties and material models

Snow is a cellular form of ice crystals bound together, which forms in the atmosphere because of the deposition of water vapor into ice. The deposition of water vapor requires the presence of a nucleus, which is present in the air in the form of dust particles. Snow consists of three different phases: ice, water, and air, with the water phase being minimal at subzero temperatures. Depending on its density, the most common types of snow are fresh snow, soft packed snow, medium packed snow, hard packed snow and slush (Janowski 1980).

There are various characteristics that need to be considered while analyzing snow material. Its hardness, type, and density are all affected by the metamorphic process. As a result of the densification process, the snow particles transform from flakes to granular particles. The moisture content of snow changes according on temperature and climate. Furthermore, when the tire moves across the snow, the material property changes. As a result of all of these variables, developing an accurate snow model is challenging.

# 2.1. Snow properties

Many researchers compiled a lot of knowledge related of snow mechanics study (Bader 1963, Mellor 1975, Mellor 1977). While main mechanical properties of snow and methods to identify them are briefly presented in the following sections, the reader is referred to comprehensive reviews in literature for more detailed treatment of snow mechanics (Shapiro et al., 1997) and of the snow measurement methods (Shenvi et al., 2022).

# 2.1.1. Snow density and mechanical properties

Snow density is an important physical property of snow and varies from 100 kg/m<sup>3</sup> for fresh snow to 600 kg/m<sup>3</sup> for snowpack subjected to melt-freeze cycles. The maximum density of snow may reach up to 900 kg/m<sup>3</sup> (ice density). The compacted snow that automobiles can experience is typically classified as having a density ranging from 370 to 560 kg/m<sup>3</sup> (Shoop et al., 2010).

Numerous research tried to quantify the macroscopic mechanical behavior of various snow types under different loading conditions and temperatures (Mellor 1975, Shapiro et al., 1997). However, no strong correlation between mechanical properties and snow density was observed (Mellor 1975). As a result, it seems that density alone is insufficient to completely characterize the mechanical behavior of snow (Voitkovsky et al., 1975, Shapiro et al., 1997), including compressive strength, and intergranular bonding (Fukue 1979, Shapiro et al., 1997).

Snow deformations are primarily controlled by grain rearrangements, which are caused by bond failure and creation. This kind of deformation occurs when slab avalanches are released (Schweizer 2003), when a snow profile is characterized using an indenter (Schneebeli et al., 1999), or during tire- snow ground interaction (Schneebeli et al., 1999). If the snow has been compressed, well-bonded and of high density, then even comparatively large stresses can be sustained without considerable deformation. In these cases, linear relations are possibly applicable over a relatively large range of stresses (Abele and Gow 1976, Shapiro et al., 1997).

The relationship between the uniaxial compressive strength and density of snow were investigated by different studies (Kinosita 1967, Mellor 1975, Abele 1990). In compression process, as density increases, the compressive strength of snow increases (Fig. 1). A similar trend was observed for natural densification of snow, as density increased (100–600 kg/m³) the compressive strength of snow increases (10<sup>-4</sup> to 10<sup>-1</sup> MPa). By comparison (Fig. 1), the strength of natural and compacted snow (Fig. 1: Plot 1, 3, 4) is obviously higher than that the strength of snow produced

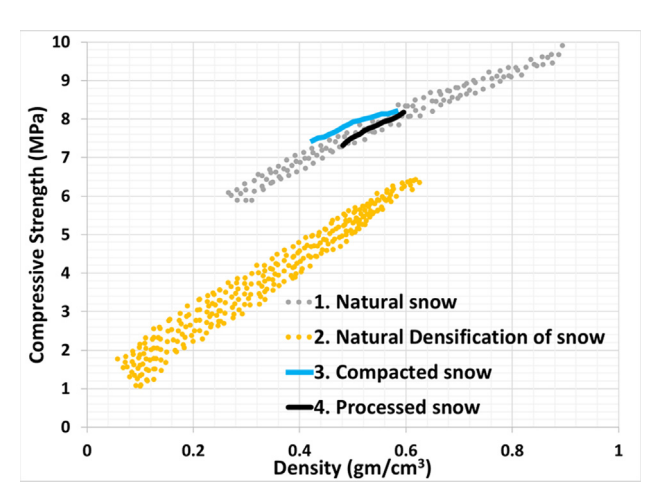


**Fig. 1.** The relationship between the uniaxial compressive strength and density from different studies (1) compacted snow (Wang et al., 2021), (2) processed snow (Abele, 1990), (3) natural snow (Kinosita, 1967), (4) Natural densification of snow deposits (Mellor, 1975). Redrawn in agreement to plot in (Wang et al., 2021).

by the slow compression of snow under natural conditions (Fig. 1: Plot 2). The ultimate uniaxial compressive strength of compacted snow was also increasing at higher snow densities and lower temperatures (-5 °C to -20 °C, Fig. 2). The rate of change in ultimate uniaxial compressive strength is low in the density range of 350 to 450 kg/m³, while it is greater in the density range of 450 to 600 kg/m³(Wang et al., 2021).

# 2.1.2. Young's modulus of snow

Young's modulus of snow is an important parameter for tire traction (Choi et al., 2012). However, determination of the elastic modulus of snow is challenging (Mellor 1975), mainly due to complex snow properties, such as its strain-rate dependency, and microstructural effect. Many researchers used uniaxial compression test, micro-computed tomography (uCT) and FEM to calculate elastic modulus (E) of snow (Köchle and Schneebeli 2014, Wautier et al., 2015, Srivastava et al., 2016). Generally, uniaxial compression experiments conducted at very low strain rates (less than 4x10<sup>-4</sup> per sec), the elastic modulus was reported in the range of 0.2 to 20 MPa (Fig. 3: Plot 1) for density between 100 to 350 kg/ m<sup>3</sup> (Mellor 1975). Similar values were observed from quasi-static triaxial compression tests with strain rate less than 10<sup>-3</sup> per sec (Fig. 3: Plot 5 (Scapozza 2004)). The complex microscale geometry of snow samples on a millimeter scale are reconstructed from μCT scans (Köchle and Schneebeli, 2014; Lundy et al., 2002) Then the FE models of these samples are derived, and a porous cohesive material is assigned using ice material properties (Sanderson, 1988). Then, the effective elastic modulus is determined based on FE axial compression simulations.

In dynamic loading experiments, the higher values of Young's modulus (from 20 to 70 MPa) were determined at high strain rates (greater than  $10^{-2}$  per sec) for snow densities ranging from 210 to 360 kg/m³ (Fig. 3: Plot 3 (Sigrist 2006)). The elastic modulus values calculated from the micro-computed tomography ( $\mu CT$ ) were found in the range of 14 to 340 MPa and were close to the values (range of 11 to 275 MPa) which are obtained from the acoustic wave propagation experiments (AC) (Fig. 3: Plot 8 and 9). On the other hand, Snow Micro- Pen Measurements (SMP) values were ranging from 0.6 to 2.4 MPa, which were more than an order of lower magnitude. (Fig. 3: Plot 10).

The effective elastic modulus of the snow slab and the specific fracture energy of the underlying weak layer were reported for 80 different snowpack configurations (Van Herwijnen et al.,

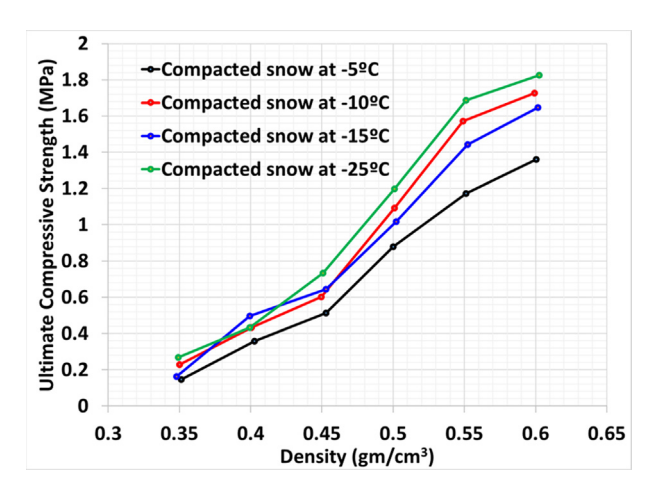


Fig. 2. The relationship between the Ultimate uniaxial compressive strength and density of compacted snow. Redrawn in agreement to plot in (Wang et al., 2021).

2016). The effective elastic modulus were ranging from 0.08 to 34 MPa and showed to follow a power law variation relative to snow density (Fig. 3: Plot 4) (Van Herwijnen et al., 2016).

$$E(\rho) = 0.93 \rho^{2.8} \tag{1}$$

On other hand, the elastic modulus was fit to an exponential relationship relative to snow density when snow density was in a range of 250 kg/m<sup>3</sup> up to 450 kg/m<sup>3</sup> (Köchle and Schneebeli 2014).

$$E(\rho) = 6.0457e^{0.011\rho} \tag{2}$$

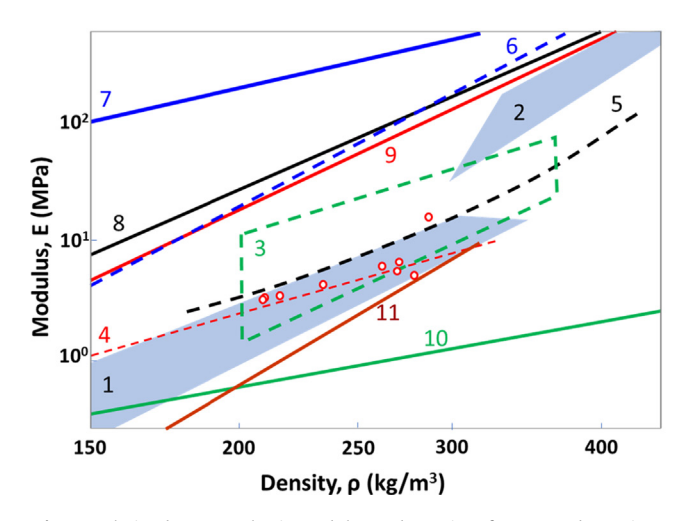
The model reported (Camponovo and Schweizer, 2001) based on laboratory measurements performed at 1 Hz (Fig. 3: Plot 11) and (Fig. 3: Plot 12) estimates from SMP measurements (red circles) (Schweizer, 2011).

In conclusion, different values of Young's modulus were reported for the same density range (Table 1 and Fig. 4). This inconsistency could be explained by the differences in experimental methodology, as well as variation in strain rate and snow temperature used in the experimental studies. Furthermore, the empirical relationship between density and elastic modulus changes depending on the assumptions and theories used in each study (Eqs. (1) and (2)).

# 2.2. Snow material models

A wide range of material models, including elastic, elastic–plastic, and elastic-visco-plastic, have been used to model the snow and its interaction to tire loads. The linear elastic approach for snow modelling was used in several studies (Smith 1971, Habermann et al., 2008, Heierli and Zaiser, 2008) with Young's modulus of snow ranging from 0.15 to 7.5 MPa, density from 100 to 400 kg/m³, and Poisson's ratio between 0.1 and 0.3 (Table 2). Since snow is complex in nature, material models with higher complexity than simple elastic model were tried as well.

The elasto-plastic material model of snow based on Capped Drucker-Prager model was used to simulate plate sinkage tests and the Cam-Clay yield model was used to simulate shear box tests (Seta et al., 2003). Many studies used Drucker-Prager cap model for modelling fresh snow as well as compacted snow. For low density snow (density from 200 to 250 kg/m<sup>3</sup>) the material cohesion values were varied from 5 to 30 kPa and internal friction angle was 22.52°. (Shoop 2001, Haehnel and Shoop 2004). For compacted snow (density 500 kg/m<sup>3</sup>), the material cohesion value was 130 kPa and internal friction angle was ranging from 60 to 70° (Mundl et al., 1997, Choi et al., 2012)(Table 3). Similarly, the Cam-Clay yield model was used also used for modelling snow behavior in few studies (Salm 1982, Narita 1984). The viscoplastic characteristic of snow, representing by its ratedependency, showed to play an important role in the long-term densification of the snowpack mostly through microscale ice skeleton deformation. The mechanisms of deformation and degradation of the intergranular linkages are assumed to be connected to snow viscosity and yielding. The formation of intergranular bonds may be represented at the macroscopic scale (Nova 1992). Many researchers have used different strain rate values in their studies (Desrues et al., 1980, Meschke et al., 1996, Moos et al., 2003, Scapozza and Bartelt, 2003a, Scapozza and Bartelt, 2003b, Cresseri and Jommi 2005, Cresseri et al., 2010). Depending on the strain rate, snow shows two different kinds of mechanical behavior (Schulson and Duval 2009). Large deformations at high strain rates (greater than 10<sup>-4</sup> per sec) are primarily exhibits snow bond failures and grain rearrangements, whereas at very low strain rates (less than 10<sup>-5</sup> per sec) snow exhibits visco-plastic behavior. The important parameters that are required to generate the viscoplastic model of snow are listed in Table 4. As density of snow sample changes, the value of shear modulus changes, however, very little change in the value of consolidation index & swelling recompression index was observed.



Data from Literature

- 1. Shapiro, 1997
- 2. Shapiro, 1997
- 3. Sigrist, 2006
- 4. Van Herwijnen et al., 2016
- 5. Scapozza, 2004
- 6. Kochle and Schneebeli, 1999
- 7. Wautier, 2015
- 8. μCT (Gerling, 2017)
- 9. AC (Gerling, 2017)
- 10. SMP (Gerling, 2017)
- 11. Camponova, 2001
- 12. Schweizer, 2011- o

Fig. 3. Relation between Elastic Modulus and Density of Snow. Redrawn in agreement to plot in mentioned references.

Table 1 Selection of previous studies reporting the elastic modulus (E) of seasonal snow by mechanical testing, finite element simulations (FEM) of 3-D micro-computed tomography ( $\mu$ CT) (Reuter et al., 2019).

Contribution	Method	Strain rate (s <sup>-1</sup> )	N	Density (kg/m³)	Temperature (°C)	Young's Modulus E (MPa)
(Mellor 1975, Cresseri et al., 2010)	Various	10 <sup>-3</sup> to 10 <sup>-2</sup>	_	$\approx 100$ to $500$	-25  to  -6.5	0.1 to 1000
(Köchle and Schneebeli 2014)	μCT, FEM	-	89	100 to 500	-	1 to 1000
(Cresseri et al., 2010, Wautier et al., 2015)	μCT, FEM	-	31	100 to 550	-	45 to 3600
(Srivastava et al., 2016)	μCT, FEM	_	25	97 to 533	_	1 to 1800
(Scapozza 2004)	Uniaxial compression test	10 <sup>-6</sup> to 10 <sup>-3</sup>	$\sim\!\!200$	180-440	-18.7  to  -1.8	3 to 120

Strain rate, number of experiments (N), average density and snow temperature are listed if reported.

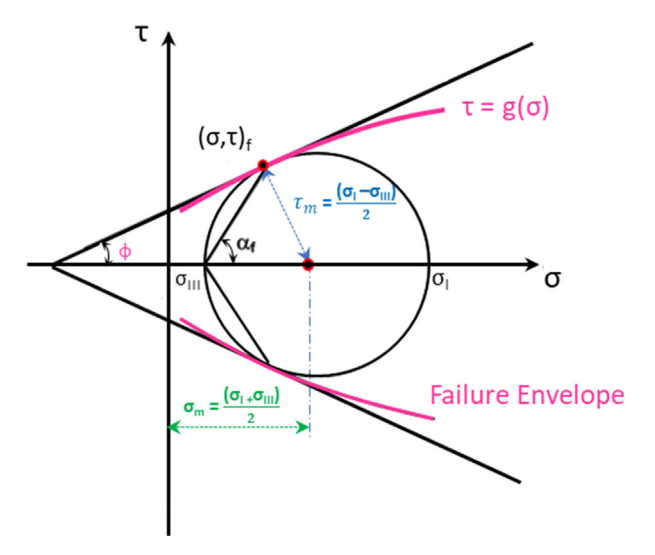


Fig. 4. Mohr diagram and failure envelopes. Redrawn in agreement to the schematic in (Labuz and Zang, 2012).

## 2.3. Snow failure models

Material failure theories tried to predict the conditions under which the solid materials fail. The material failure, defined as losing the load carrying capacity under external loads which are specified in ductile and brittle materials by the initiating of yielding and by fracture, respectively. Several failure theories, used mostly in soil mechanics, were tried to be used in predicting snow failure and are reviewed in this section.

## 2.3.1. Mohr-Coulomb failure criterion

The Mohr-Coulomb failure criteria has been extensively used to geotechnical engineering. This failure criterion is usually combined with an elastically-perfectly plastic material model called sometime, Mohr-Coulomb material model. The failure is regulated by the maximum shear stress and this failure shear stress is a function of the normal stress. This may be shown by drawing Mohr's circle for states of stress at failure in terms of the principal stresses (maximum and minimum). The best straight line that touches these Mohr's circles is the Mohr-Coulomb failure line. This failure crite-

rion is a set of linear equations between normal stress  $\sigma$  and shear stress  $\tau$  describing the conditions for which an isotropic brittle material will fail (Labuz and Zang, 2012). Thus, the Mohr-Coulomb criterion can be written as.

$$|\tau| = C + \sigma \tan \phi \tag{3}$$

From Mohr's circle,  $\tau = \tau_m \cos \phi$ ,  $\sigma = \sigma_m + \tau_m \sin \phi$ ,  $\tau_m = \frac{(\sigma_I - \sigma_m)}{2}$  and,  $\sigma_m = \frac{(\sigma_I + \sigma_m)}{2}$  where  $\tau$  is the shear stress,  $\sigma$  is the normal stress and two material constants included in the criteria are c is the cohesion of the material and  $\phi$  is the angle of internal friction with coefficient of internal friction  $\mu = tan\phi$ . In the Mohr diagram (Fig. 4), this criterion is represented by a straight line inclined to the  $\sigma$  axis by the angle  $\phi$ . By plotting a Mohr circle tangent to the line and applying trigonometric relations, the alternative form of eqn. (3) in terms of principal stresses is obtained.

$$(\sigma_I - \sigma_{III}) = (\sigma_I + \sigma_{III}) \sin\phi + 2S_0 \cos\phi \tag{4}$$

Mohr's failure criteria may be also expressed as:

$$\tau_m = f(\sigma_m) \tag{5}$$

The Mohr envelope may be created on the plane (Fig. 4), using the relationship provided by Eq. (5), and failure occurs if the stress state at failure, the circle of diameter  $(\sigma_I - \sigma_{III})$  is tangent to the failure envelope,  $\tau = g(\sigma)$ .

Therefore, Coulomb's criteria are equal to the assumption of a linear Mohr envelope, as shown in Eq. (6).

The Mohr-Coulomb approach is generally used for brittle materials to find the properties of cohesion and internal friction angle, and it had been extensively utilized to study snow-tire interactions (Bekker 1969, Lever et al., 2006, Choi et al., 2012). For example, it has been used to define the failure of weak snow layers (Gaume et al., 2013; Podolskiy et al., 2014; Chiaia et al., 2009). Many researchers used the elastoplastic model with Mohr-Coulomb failure criterion (Dytran 2002, Seta et al., 2003) and some studies used elasto-plastic model of snow interface with shear softening using Mohr-Coulomb rupture criterion (Gaume et al., 2012). Similarly, 2-D and 3-D finite element soil models was developed using an elastic-plastic material model following the Mohr-Coulomb yield criterion described by cohesion stress and friction angle (Hambleton and Drescher 2008, Hambleton and Drescher 2009).

**Table 2**Snow material properties used in the finite element model for elastic model.

Contribution	Young's Modulus, E (MPa)	Density, $\rho$ (kg/m <sup>3</sup> )	Poisson's ratio
(Smith 1971, Cresseri et al., 2010)	0.2 to 1.2	100 to 400	0.1 to 0.3
(Smith 1972, Cresseri et al., 2010)	0.2	127, 227, 310	0.2
(Habermann et al., 2008)	0.15 to 7.5	100 to 270	0.25
(Sigrist 2006)	5, 20	250, 300	-

Table 3

Mohr Coulomb Model							
Contribution	Density ( $\rho$ ) kg/m <sup>3</sup>	Material cohesion (C) kPa	Material angle of friction $(\phi)$				
(Seta et al., 2003, Cresseri et al., 2010)	200	40	60°				
	520	16	31°				
Drucker-Prager cap model	Density (ρ) kg/m³	Material cohesion (C) kPa	Material angle of friction (φ)	Can ecc	entricity	naramete	r (R)
(Shoop 2001)	200 to 250	5 to 30	22.52°	-	to 1.1E-4	paramete	(K)
(Mundl et al., 1997)	500	130	60° to 70°	_			
(Haehnel and Shoop 2004)	200	5	22.528°	0.02			
(Choi et al., 2012)	350	85	65	_			
	500	130	70	_			
Cam-Clay model							
Contribution	Density (ρ) kg/m³	Shear modulus (G) MPa	λ	k	N	M	q <sub>o</sub> (MPa)
(Meschke, Liu, and Mang 1996)	400	7.5	0.38	0.015	3.05	2.88	0.07

 $<sup>\</sup>lambda$ - consolidation index, k- swelling recompression index, N- specific volume at unit hydrostatic pressure, M- slope of critical state line and  $q_0$ - Preconsolidation pressure.

**Table 4**Snow material properties used in the finite element model for Visco-plastic model.

Contribution	Density $(\rho) \text{ kg/m}^3$	Shear modulus (G) MPa	consolidation index $(\lambda)$	swelling recompression index (k)	Strain rate ψ (per <i>sec</i> )
(Meschke, Liu, and Mang 1996; Cresseri et al., 2010)	400	12.426	0.35	0.02	4.2x10 <sup>-6</sup>
(Scapozza and Bartelt, 2003a, Cresseri et al., 2010)	360	8.179	0.4	0.02	2.6x10 <sup>-5</sup>
(Moos et al., 2003, Cresseri et al., 2010)	314	5.287	0.35	0.015	3.46x10 <sup>-6</sup>
(Scapozza and Bartelt, 2003a, Cresseri et al., 2010)	272	4	0.35	0.02	1.06x10 <sup>-5</sup>
(Desrues et al., 1980, Cresseri et al., 2010)	200	2.114	0.35	0.02	1.0x10 <sup>-5</sup>
(Cresseri and Jommi 2005, Cresseri et al., 2010)	200 to 550	4	0.35	0.02	4.2x10 <sup>-6</sup>

## 2.3.2. Drucker-Prager failure criterion

The Drucker–Prager failure criterion is a pressure-dependent model used to determine whether a material has failed or has undergone plastic yielding. The criteria were developed to address plastic deformation of soil and applies to materials such as rock, concrete, polymers, foams, and other pressure-dependent materials like compacted snow. This failure criteria are a three-dimensional pressure-dependent model for calculating the stress state at which the rock achieves its ultimate strength. The criterion assumes that the octahedral shear stress at failure depends linearly on the octahedral normal stress through material constants. As an extension of the Mohr–Coulomb criteria for soils, the Drucker–Prager failure criterion was established and it can be expressed by eqn. (6) (Drucker and Prager 1952).

$$\sqrt{J_2} = \lambda I_1' + k \tag{6}$$

where  $\lambda$  and k are material constants,  $J_2$  is the second invariant of the stress deviator tensor and  $I_1^{'}$  the first invariant of the stress tensor, and are defined as  $I_1^{'} = \sigma_1^{'} + \sigma_2^{'} + \sigma_3^{'}$  and  $J_2 = \frac{1}{6}[(\sigma_1^{'} - \sigma_2^{'})^2 + (\sigma_1^{'} - \sigma_3^{'})^2 + (\sigma_3^{'} - \sigma_3^{'})^2]$ 

 $\sigma'_1, \sigma'_2, \sigma'_3$  are the principal effective stresses.

The D-P failure criterion, can be expressed in terms of octahedral shear stress,  $\tau_{oct}$ , and octahedral normal stress,  $\sigma_{oct}$  by eqn. (8).

$$\tau_{oct} = \sqrt{\frac{2}{3}} (3\lambda \sigma'_{oct} + k) \tag{7}$$

where  $\sigma'_{oct}=\frac{1}{3}I'_1$  and  $\tau_{oct}=\sqrt{\frac{2J_2}{3}}$  The D-P criterion can thus be considered as per Nadai's criterion (Addis, 1993; Chang and Haimson, 2000; Nadai, 1950; Yu, 2002) which states that the mechanical strength of brittle materials takes the form of eqn. (8).

$$\tau_{oct} = f(\sigma'_{oct}) \tag{8}$$

where f is function that increases monotonically. The criterion expressed in. Eq. (6), describes a right-circular cone in the stress space when  $\lambda$ >0, or a right circular cylinder when  $\lambda$ =0; hence the intersection with the  $\pi$ -plane is a circle (Fig. 5). The value of  $\lambda$  and k can be calculated from triaxial test by plotting the values of  $I_1$  and  $\sqrt{J_2}$  space. The values of  $\lambda$  and k can also be determine from expression in terms of internal friction angle ( $\phi$ ) and cohesion intercept (c) using eqn. (9) and (10).

$$\lambda = \frac{2\sin\phi}{\sqrt{3}(3-\sin\phi)}\tag{9}$$

$$k = \frac{6c\cos\phi}{\sqrt{3}(3-\sin\phi)}\tag{10}$$

If the cohesion and internal friction angle of the MC failure theory are known, the constants of the DP failure criterion can be determined, and vice versa. (Jiang 2011, Lee 2016). These criteria are commonly used in geotechnical engineering to calculate failure strength and be utilized to determine plastic potential in a continuum damage mechanic model. Drucker–Prager plasticity model is used to calculate pressure-sinkage relationship of snow model (Lee 2009, Lee 2013). In order to represent snow behavior correctly, it is necessary to, the multi-surface Drucker–Prager plasticity model is employed (Meschke 1995, Rooney et al., 2002). Furthermore, some researcher used Drucker–Prager model for representing weak layer of a slab and interface with shear softening. (Gaume, 2011).

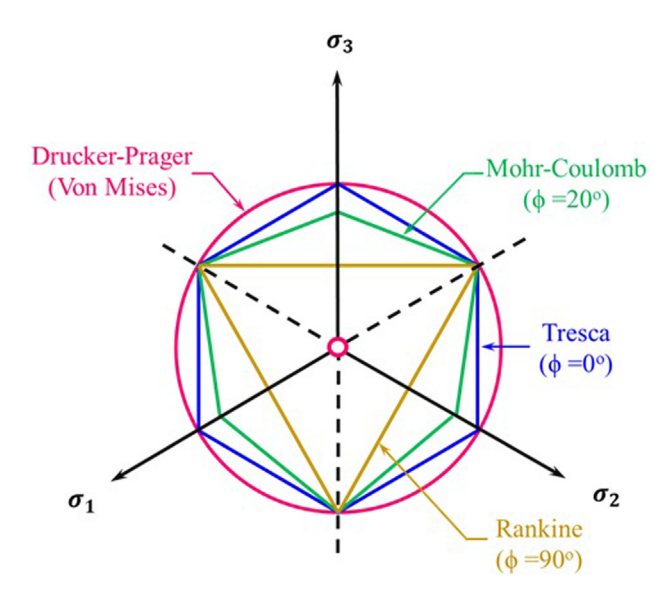


**Fig. 5.** Drucker–Prager and Mohr–Coulomb failure criteria in deviatoric space. Redrawn in agreement to the schematic in (HKS, 1998, Shoop, 2001).

# 2.3.3. Modified-Drucker Prager with cap failure criterion

The Drucker Prager with Cap (DPC) plasticity model has been improved and extended over the years (Chen and Mizuno, 1990; Sandler, 2002). This criterion represents the material behavior subjected to the permanent deformation (Bažant 1985, ABAQUS 2003) and it is capable of accounting for both compaction and shear failure, as well as a transition zone between the two failure regimes (Han et al., 2008) (Fig. 6a). It comprises of three parts: 1-a linear shear failure surface represents increasing shear stress with increasing mean stress which provides dominantly shearing flow; 2- a curved "cap" intersecting both the shear failure surface which provides an inelastic hardening mechanism to signify plastic compaction and 3- the mean stress axis; and a transition surface allowing a smooth intersection between the cap and failure surfaces. In the equivalent pressure stress- deviatoric stress plane (p-q plane), the equations describing these three surfaces are expresses as.

1. Shear failure surface, 
$$F_s = q - ptan \phi - C = 0$$
 (11)

where q is the Von Mises equivalent stress or deviatoric stress measure, p is hydrostatic pressure stress,  $\phi$  is the angle of friction and c is the material cohesion.

# 2. Compression Cap =

$$F_{c} = \sqrt{(p - p_{a})^{2} + \left[\frac{Rq}{1 + \infty - \infty / \cos\phi}\right]^{2}} - R(C + p_{a} \tan\phi) = 0 \quad (12)$$

where  $\alpha$  is a numeric parameter that defines a smooth transition yield surface intersection between the cap and failure surfaces, R is the ratio between the horizontal axis and the vertical axis of the elliptical cap, and  $p_a$  is an evolution parameter for volumetric plastic, strain-driven hardening or softening of the cap.

# 3. Transition surface =

$$F_t = \sqrt{(p - p_a)^2 + [q - (1 - \frac{\alpha}{\cos\phi})(C + p_a tan\phi)]^2}$$

$$-\alpha (C + p_a tan\phi) = 0$$
(13a)

The Mohr-Coulomb yield condition is approximated in ABAQUS (Explicit) by a modified D-P yield condition (ABAQUS, 2006), which has a corresponding associated or unrelated flow potential. This

model was used to simulate the behavior of natural fresh snow (Shoop 2001). The plastic flow is defined by an elliptical potential surface (Fig. 6b). Flow which is normal to the surface associative in the cap region; therefore, the flow surface equation is similar to the equation for the cap yield surface.

In the transition and shear regions, the flow is non-associative (the flow potential is not perpendicular to the failure surface) and is defined by the equation (13b).

Flow potential shear surface =

$$G_s = \sqrt{\left[(p_a - p)tan\phi\right]^2 + \left[\frac{t}{1 + \infty - \infty/cos\phi}\right]^2} = 0$$
 (13b)

# 2.3.4. Cam-clay and modified cam-clay failure criterion

Cam-Clay (CC) and Modified Cam-Clay (MCC) models are widely used to simulate the behavior of soil and soft clay (Borja and Lee 1990, Borja 1991, Hashash and Whittle 1992, Simo and Meschke 1993, Callari et al., 1998). The CC model assumes the terrain as an isotropic elastoplastic material, which it is not influenced by creep. When the terrain is snowy, these assumptions may be in direct conflict, and the model may have convergence challenges. Hence very few studies used this model to capture snow behavior (Meschke et al., 1996).

The MCC model can be thought of as an elastoplastic model that gradually hardens. The effect of yield surface shape and plastic potential surfaces, as well as performing undrained analysis, are two common errors in the application of the MCC model (Potts and Zdravkovic 1999). Both models assume that a normal compression line and various unloading–reloading lines may be used to characterize the relationship between the specified volume and the average normal stress. They also demand that the Poisson's ratio or the material's shear modulus be specified (Borja and Lee 1990, Borja 1991, Peinke et al., 2020).

Both CC and MCC models are elastic plastic strain hardening models based on Critical State theory and the assumption that the mean stress and void ratio have a logarithmic relationship. Researchers at Cambridge University created the first critical state model for understanding the behavior of soft soils such as cam clay and modified cam clay (Roscoe 1968). These models address three fundamental aspects of soil behavior: strength, compression or dilatancy (the volume change caused by shearing), and the Critical State, when soil materials may undergo unlimited deformation without any changes in stress or volume. A significant portion of the volume occupied by a soil mass consists of voids that may be covered by fluids (primarily air and water). Thus, soil deformations are accompanied by significant and irreversible change in volume. A major benefit of the cap plasticity models, a class to which the CC and MCC formulations belong, is their capability to model changes in volume more accurately.

The state of a soil sample is defined by three parameters in critical state mechanics: Effective mean stress p', Deviatoric (shear stress) q', and Specific volume v. The mean stress can be evaluated under general stress conditions in terms of principal stresses p'  $\sigma'_1$ ,  $\sigma'_2$  and  $\sigma'_3$  as.

$$p' = \frac{1}{3}(\sigma'_1 + \sigma'_2 + \sigma'_3) \tag{14}$$

and triaxial shear stress is expressed as.

$$q' = \frac{1}{\sqrt{2}} \sqrt{\left(\sigma'_1 - \sigma'_2\right)^2 + \left(\sigma'_2 - \sigma'_3\right)^2 + \left(\sigma'_3 - \sigma'_1\right)^2} \tag{15}$$

Virgin Consolidation Line and Swelling Lines can be represented when a sample of soft soil is gradually compressed under isotropic stress conditions  $p' = \sigma'_1 = \sigma'_2 = \sigma'_3$  and under perfectly drained

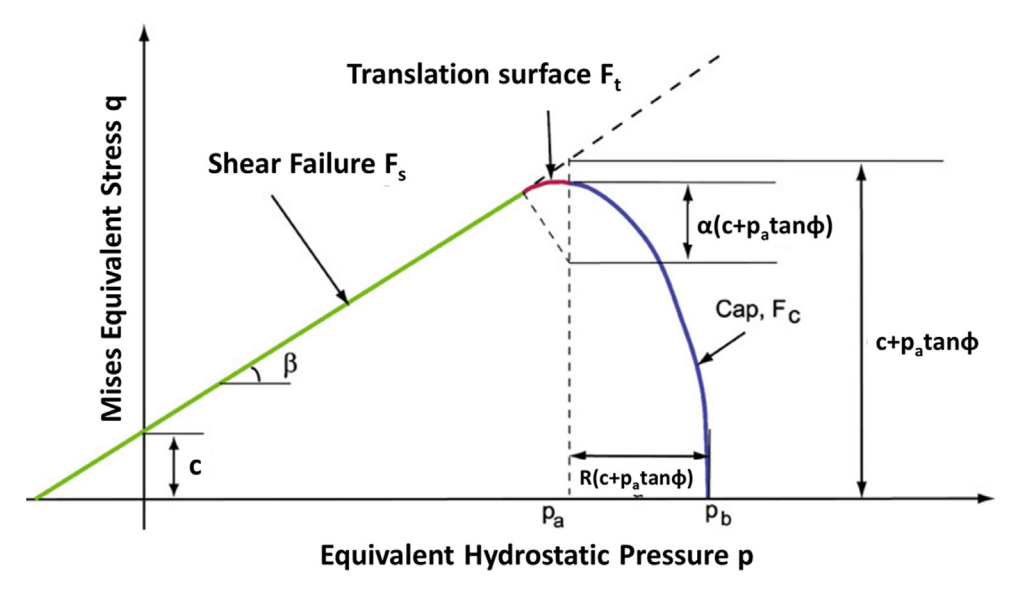


Fig. 6a. Drucker-Prager Cap model: yield surface in the p-q plane. Redrawn in agreement to the schematic in (Shoop, 2001).

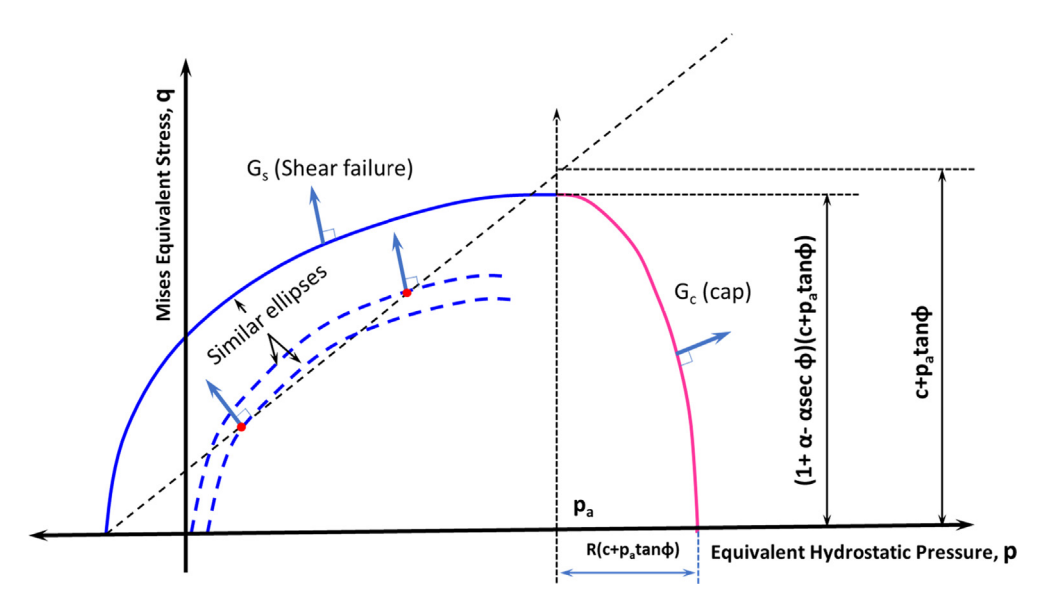


Fig. 6b. Modified Drucker-Prager cap flow potential in the p-q. Redrawn in agreement to the schematic in (Shoop, 2001).

conditions, the relationship between specific volume, v, and lnp' consists of a straight virgin consolidation line and a set of straight swelling lines (Fig. 7a).

The virgin consolidation line is expressed by the equation.

$$v = N - \lambda' \ln p' \tag{16}$$

and swelling line is expressed by the equation.

$$v = v_{\rm s} - \kappa lnp' \tag{17}$$

where  $\kappa$ ,  $\lambda'$  and N are characteristic properties of a particular soil.  $\kappa$  is the slope of swelling line in  $\nu$  space,  $\lambda'$  is the slope of the normal compression (virgin consolidation) line or the critical state line in  $\nu - lnp'$  space. N is known as the specific volume of normal compression line at unit pressure,  $\nu - lnp'$  and  $\nu_s$  differs for each swelling line, depends on the loading history of a soil (Fig. 7a).

Sustained shearing of a soil sample eventually results in a situation in which more shearing is possible without affecting the stress or volume of the soil. This is referred to as the critical state, which occurs when the soil distorts at a consistent rate. This state

is characterized by the Critical State Line (CSL). The location of this line relative to the normal compression line (Fig. 7b).

CSL is parallel to the virgin consolidation line in  $v-lnp^{'}$  space. The parameter  $\Gamma$  is the specific volume of the CSL at unit pressure. Like N, its value depends on measurement units. For the CC model the relationship between the parameter N of the normal compression line and  $\Gamma$  can be expressed by.

$$\Gamma = N - (\lambda - \kappa) \tag{18}$$

Similarly, for the MCC model the relationship can be expressed as.

$$\Gamma = N - (\lambda - \kappa) \ln 2 \tag{19}$$

 ${\bf q}$ , CC, and MCC soils all behave elastically when subjected to increasing triaxial shear loads until a yield value of  ${\bf q}$  is reached. Therefore, yield values for CC Model can be expressed as.

$$q + Mp \ln \left(\frac{p'}{p'_0}\right) = 0 \tag{20}$$

Similarly, yield values for MCC Model can be expressed as.

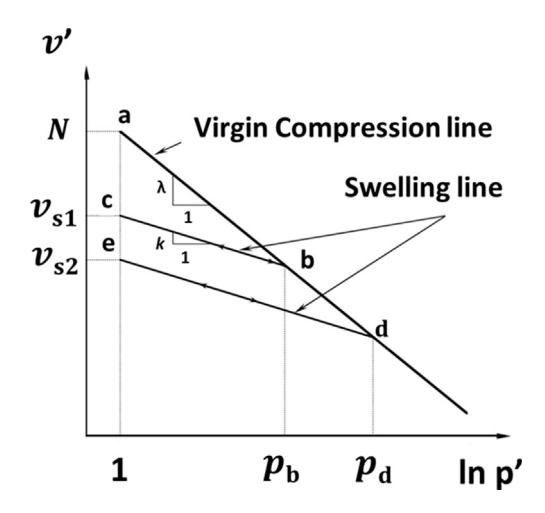


**Fig. 7a.** Behavior of soil sample under isotropic compression. Redrawn in agreement to the schematic in (Rocscience).

$$\frac{q^2}{p'^2} + M^2 \left( 1 - \frac{p'}{p'_0} \right) = 0 \tag{21}$$

In space, the CC yield surface is a logarithmic curve, while the MCC yield surface plots as an elliptical curve (Fig. 7c). yield stress or pre-consolidation pressure parameter controls the size of the yield surface and is different for each swelling line. The parameter M is the slope of the CSL in space. An important characteristic of the Critical Straight Line is that it crosses the yield curve at the point at which the maximum value of q is achieved.

# 3. Modeling of tire-snow interaction

Many numerical methods were proposed in literature to investigate compacted snow-tire interaction such as analytical and semi-analytical methods, mesh-based methods and particle-based methods. These methods are reviewed in the next sections.

# 3.1. Analytical/semi-analytical methods

Analytical/semi-analytical methods are used to estimate the longitudinal traction of a tire in snow. These methods consist of mathematical approaches which are able to predict the forces and moments at the tire-snow interface (Browne 1974, Nakajima 2003, Lee et al., 2005, Lee and Liu 2006, Lee, 2011a). During tire-snow interaction, the generated longitudinal snow traction con-

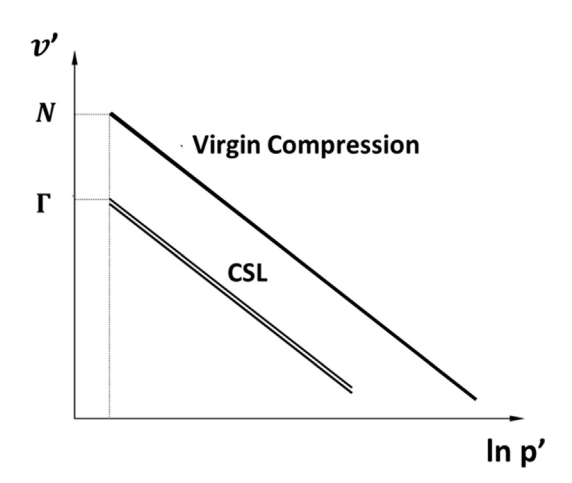


**Fig. 7b.** Location of CSL relative to virgin compression line. Redrawn in agreement to the schematic in (Rocscience).

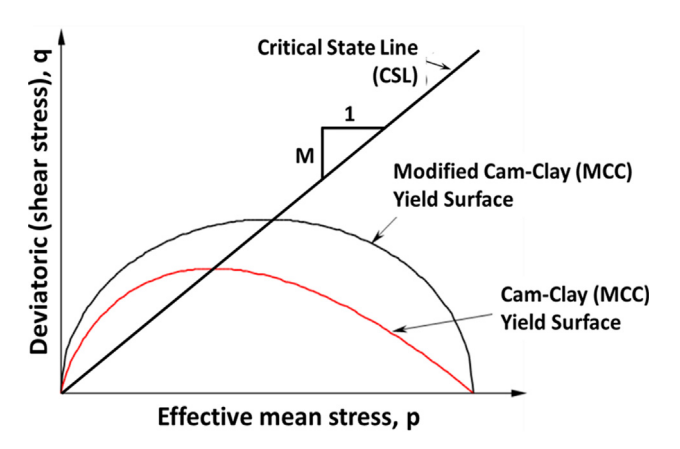


**Fig. 7c.** CC and MCC yield surfaces space. The parameter M is the slope of the CSL. Redrawn in agreement to the schematic in (Rocscience).

sists of four types of forces (Fig. 8): shear force of snow in void (space between tread blocks) (F<sub>S</sub>), frictional force between tire and snow (F<sub> $\mu$ </sub>), digging force (edge effect generated by sipes and blocks) (F<sub>D</sub>) and the braking force (F<sub>B</sub>) generated by snow compression at the leading edge. Traction at the time when a tire starts rolling is called static traction (Eqn. (22)) (Nakajima 2003).

Static tractionv(without slip) = 
$$F_S + F_{\mu} + F_D - F_B$$
 (22)

When the slip ratio becomes 1.0 (high slip),  $F_S$  and  $F_B$  does not generate a force, so the equation of traction with a 1.0 slip ratio becomes:

Traction (with 1.0 slip ratio) = 
$$F_{\mu} + F_{D}$$
 (23)

The static traction of tire was predicted using Eq. (22) and compared to experimental measurements. As the measurement was taken one day after the snowfall, the mechanical properties of snow, such as compression and shear strength, were taken from reference (Muro and Yong 1980). The prediction of traction agreed with experimental results as well.

A traditional rigid wheel terra-mechanics model (Wong 1993) was adapted for snow by using a snow indentation model (physical model based on plasticity) commonly used for soils. These models are depth-dependent whereas most soil models are depth-independent. This method was useful for predicting tire sinkage as a function of longitudinal slip, tire vertical load, snow depth, hardness and coefficient of rolling resistance (Lee 2009, Lee et al., 2010).

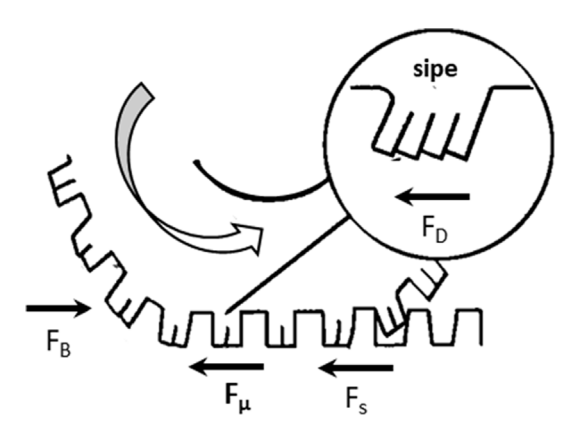


Fig. 8. The components of longitudinal snow traction of a rolling tire. Redrawn in agreement to the schematic in (Nakajima 2003).

The sinkage of snow z at a typical point at an angle  $\theta$  (Fig. 9) on the tire–snow interface is related to the exit angle  $\theta_0$  by.

$$z(\theta) = r(\cos\theta - \cos\theta_0) \tag{24}$$

where r is the radius of tire. The vertical force  $F_z$  acting on the tire can be related to the normal stress  $(\sigma_n)$  and shear stress  $(\tau)$  at the interface by:

$$F_z = b.r \left[ \int_0^{\theta_0} \sigma_n(\theta) cos\theta \, d\theta + \int_0^{\theta_0} \tau(\theta) sin\theta \, d\theta \right] \tag{25}$$

where b is the width of the contact patch of the tire.

The applied torque  $(M_y)$  is expressed as:

$$M_{y} = r.b \left[ \int_{0}^{\theta_{0}} \tau(\theta) \, d\theta \right] \tag{26}$$

The motion resistance (R<sub>x</sub>), always positive, is defined as.

$$R_{x} = r.b \left[ \int_{0}^{\theta_{0}} \sigma_{n}(\theta) sin\theta \, d\theta \right]$$
 (27)

The c  $(F_{\tau x})$ , which can be positive or negative, is defined as:

$$F_{\tau x} = r.b \left[ \int_{0}^{\theta_0} \tau(\theta) \cos\theta d\theta + f_{rr} + F_z \right]$$
 (28)

where  $f_{rr}$  is the rolling resistance that adds to the traction force. The drawbar pull  $(F_x)$  is defined as:

$$F_{x} = F_{\tau x} - R_{x} \tag{29}$$

Parametric studies of the model indicated that normalized motion resistance and traction against the normal force decrease with the increase of the normal force (Lee 2011b). In addition, it was observed good correlation to test data for some models (e.g. with a larger coefficient of rolling resistance) and the range of tire sinkage from the model matches well experimental test data. However, predicted slips associated has poor correlation with test data which shows that a better shear stress-shear displacement submodel is needed. Furthermore, the analytical deterministic tiresnow interaction model was converted into a stochastic one which show a better agreement to test data (Lee 2013).

The conventional brush model is a well-known approach to the modeling of tire-road interaction. This simple model use small brush elements, linear elastic and independent bristles. Additionally, the brittles' properties allow them to adhere to the front part

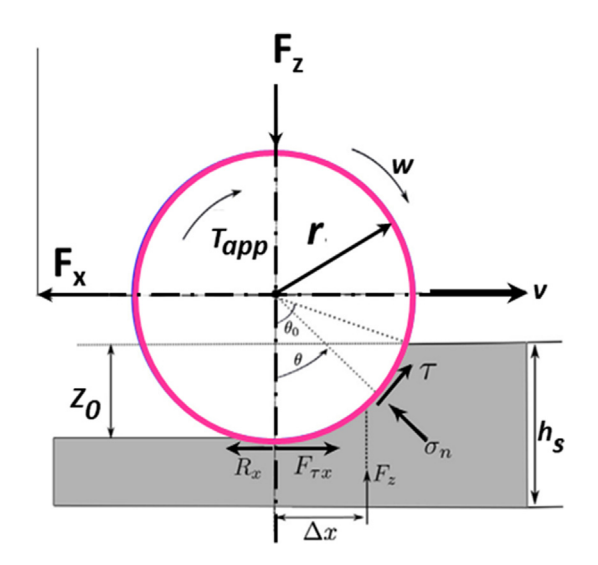


**Fig. 9.** Schematic of tire–snow interaction. Redrawn in agreement to the schematic in (Lee 2013).

of the contact patch and to slide in the rear. Snow accumulates in the tire patterns' voids and sipes when driving on snowy roads, generating snow-road surface forces. The conventional brush model (Bakker et al., 1989, Svendenius 2003) represents only the road-tire interaction without taking the tread pattern into consideration. Therefore, a double interaction brush model (Kusachov et al., 2019) was developed to represent an extra interaction between the packed snow in the voids of tire. This approach incorporates snow-shearing forces into a tire model using the brush model theory and it showed better match of test data compared with the single interaction models over a large slip range.

#### 3.2. Finite element methods

The Finite Element Method (FEM) is a widely used numerical analysis method for simulation of snow-tire interaction (Zienkiewicz et al., 2005, Podolskiy et al., 2013, Rao 2017). Lagrangian or Eulerian based finite element approaches provide effective models of complex snow-tire interaction behavior (Carbone et al., 2010, Rao 2017), even though some poor performance was reported when dealing with large deformation problems associated with snow under dynamic loading conditions (Hambleton and Drescher 2008, Hambleton and Drescher 2009).

In Lagrangian based finite element method the elements deform with the material since the mesh points remain coincident with material points during the simulation. As a result, elements could become significantly deformed, especially in threedimensional problems, which may increase the error ranges. The complex interaction between the elastic tread block or tire and the inelastically deforming snow has been carried out using Lagrangian approach (Mundl et al., 1997). Good correlation was obtained between results from laboratory experiments and from numerical simulations with respect to the snow deformations and the rubber-snow friction (Mundl et al., 1997). A twodimensional FE model has been used to compute the elastic stress distribution in realistic multi-layered snow packs, but the nonlinear and time-varying properties of snow were neglected (Smith 1971, Smith 1972). In a different study (Habermann et al., 2008), a two-dimensional finite element model of a layered snowpack with plane strain conditions were performed assuming snow as homogeneous and isotropic material.

In Eulerian approach, the mesh doesn't change as the material deforms and the domain splits into several volumes to solve for the snow response. Major disadvantage of this method is the difficulty to model free boundary surface as boundary nodes cannot be matching with the element nodes and thus it can only be used when the boundaries of the distorted surface are known a priori (LeVeque 2002, Moukalled, 2016). This method is more prominent in the disciplines of fluid analysis and aerospace engineering, although the mechanisms remain consistent even for snow behavior analysis. A three-dimensional model has been developed in which the interaction between snow and a rolling tire was considered (Seta et al., 2003, Oida et al., 2005, Seta et al., 2010). FEM and FVM were used to model tire and snow (soil) respectively. The Eulerian formulation was used for snow model to simulate its complex interaction with tire tread pattern. The predicted traction force shows good qualitative agreement with the corresponding force measured on compacted snow and soil road.

The Arbitrary Lagrangian Eulerian (ALE) is a FE formulation in which the computational method is not a prior fixed in space (e.g. Eulerian-based FE formulations) or attached to material (e.g. Lagrangian-based FE formulations). ALE-based FE simulations can overcome many of the disadvantages that the traditional Lagrangian-based and Eulerian-based FE simulations have. The ALE based FEM can handle significant deformation in the computational mesh and has capability to maintain a regular mesh config-

uration and computationally economical as compared to Lagrangian and Eulerian based FEM. Hence ALE approach is widely used in the tire industry to simulate the snow-tire interaction study due to highly nonlinear behavior of snow in large deformations and contact problems. (Shoop 2001, Lee 2009, Lee, 2011b). ALE based finite element analysis was used to simulate circular plate indentation and static tire indentation for fresh snow of different depths (Lee 2009). ALE based adaptive-explicit FEA was used to study the snow-tire interaction behavior (Terziyski 2010). A modeling methodology was examined using rubber block-snow simulations in order to evaluate its applicability to snow traction simulations. The proposed procedure was also validated with test result.

In summary, Lagrangian approach showed significant errors due to large distortions of the computational domain without recourse to frequent remeshing operations. In addition, Eulerian approach has difficulties to model free boundary surface as boundary nodes may not be coinciding with the element nodes. Therefore, ALE method, which capture the advantages of both Eulerian and Lagrangian methods, show to overcome these problems and it is widely used by many researchers to investigate the snow-tire interaction.

#### 3.3. Particle based methods

In recent years particle-based methods or meshless methods are increasing its popularity in the field of computational mechanics. Particle based methods are alternative to classical FEM which provides a significant capability for tackling field-scale problems requiring large-scale deformation and post-failure of geomaterials, such as snow and soil.

Particle based methods are broadly classified as continuum methods and discrete methods (Karajan et al., 2014) (Fig. 10). In continuum methods, the material is treated as a continuous substance, ignoring individual particles. As FEM, these methods need constitutive stress-strain relationships and apply conservation of mass, momentum and energy to small regions of material. The resulting equations are solved using numerical methods similar to FEM. The most used continuum particle-based method for tire-terrain interaction is SPH (Bui et al., 2007, El-Sayegh and El-Gindy, 2018, Bui and Nguyen, 2021). In discrete methods, the particles interact with other particles or structure based on Newton's equation of motion and a contact law to resolve inter-particle contact forces. These methods require information at the particle scale such as particle size, shape and mechanical properties. These methods are very good for investigating phenomena occurring at length scale of a particle diameter but can provide poor results for modelling large scale systems. The most used discrete methods in modelling terrain is the element-discrete method (DEM) (Johnson and Hopkins 2005, Theile et al., 2020, Xu et al., 2020). The studies which applied SPH and DEM methods in tire-snow simulations are reviewed in the following sections.

# 3.3.1. Smoothed particle Hydrodynamics (SPH) method

SPH method is the oldest mesh-free method originally developed to solve astrophysical problems in three-dimensional open space (Gingold and Monaghan 1977, Lucy 1977). In time, this mesh-free particle method, based on Lagrangian formulation, became a popular method for a wide range of scientific applications. The fundamental SPH formulation illustrated in Fig. 11, a continuum field is represented by a collection of point masses (or particles), each of which occupies a specific volume of the continuum domain and carries the mass of the occupied volume.

In particle-based methods (Fig. 11-a) the density is computed by ratio of mass to volume. However, this tends to over/under resolve clustered/sparse areas. Another option that doesn't require a mesh is to build a local volume around the sampling point. This solves the clustering problem by adjusting the size of the sample volume based on the number of particles in the area. (Fig. 11-b). However, in SPH approach (Fig. 11-c), where the density is computed via a weighted sum over neighboring particles, with the weight decreasing with distance from the sample point according to a scale factor h. The SPH particle governing equations are known to be the Navier-Stokes equations and can be described in the Lagrangian state as the mass and momentum equations (Bui et al., 2008). SPH approach was used to simulate pressure-sinkage and shear-strength tests (El-Sayegh and El-Gindy, 2018). The relationship between the plate sinkage and the applied pressure was calculated. The application for a tire-snow interaction was effective in the sole previous effort of SPH for snow (El-Sayegh and El-Gindy, 2018). However, the results lacked experimental validation because the modeled snow was validated with data from the literature and thus the SPH properties were readjusted until a fair agreement between simulation and experiment was reached. More applications of SPH methods could be found in the soil-tire interaction simulations, to predict and evaluate the soil compaction after off-road tire traffic for different vertical loads on the tire (Gheshlaghi et al., 2020). In recent soil studies the SPH terrain model was calibrated using experimental results of pressuresinkage and direct shear tests (Gheshlaghi et al., 2021). The tiressoil interaction simulations were performed over different soil conditions such as dry clay, dry sandy loam, 10 % moist, 25 % moist, and 50 % moist sand soils at different operating conditions to calculate the lateral and longitudinal forces of each tire. Similar methodology can be used in the future for snow-tire interaction studies as well.

# 3.3.2. Discrete element method (DEM)

DEM method (Cundall and Strack 1979) models particulate media (e.g., soil, snow), as a discrete collection of particle which interacts through contact forces. Various linear/non-linear cohesionless contact models are used to compute the interal) forces between particles (Fig. 12). While the normal and tangential forces are usually calculated with linear elastic-spring models, the energy dissipation by particle asperities and plastic deformations are modeled using dashpot models.

A DEM approach could model snow as a matrix consisting of air, meltwater, and grains of ice with sintering effect (Kabore et al. 2021). This modelling approach was used to predict the mechanical response of snow under compression test which is dependent on initial density, strain rate, and temperature. Predicted results obtained under a different of conditions were validated with experimental test data for both micro- and macro-scale, in particular range between ductile regimes were investigated. Similarly, an inter-granular bond and collision model were proposed in DEM for snow to describe interaction on a grain-scale (Peters et al. 2021). The aim of study was to predict the mechanical behavior of ice particles under different strain rates using a unified approach. Thus, the proposed algorithm predicted the displacement of each individual grains due to inter-granular forces and torques that derive from bond deformation and grain collision. A simple but promising experimental setup, along with DEM simulations (Steinkogler et al., 2015) that successfully reproduced the different granule classes were proposed. The presented modeling approach provided more complex and real-scale modeling of flowing cohesive snow with varying properties. A microstructure-based DEM of snow has been developed and used to investigate snow behavior under mixed-mode loading (Mulak and Gaume 2019). It was shown that sintering greatly enhanced strength for pressure loading and low loading rates, while shear-dominated loading has a negligible impact on the loading rate. Depending on applied normal stress, distinct failure regimes were identified and charac-

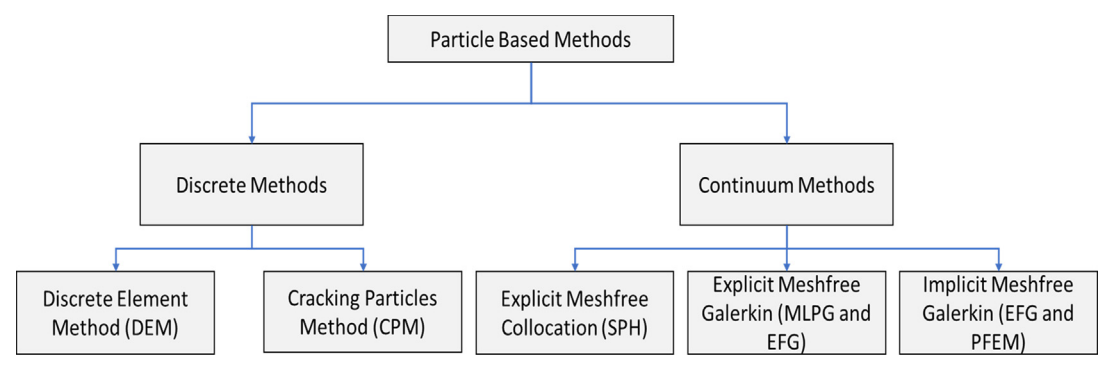


Fig. 10. Particle Based Methods. Redrawn in agreement to the schematic in (Karajan et al., 2014).

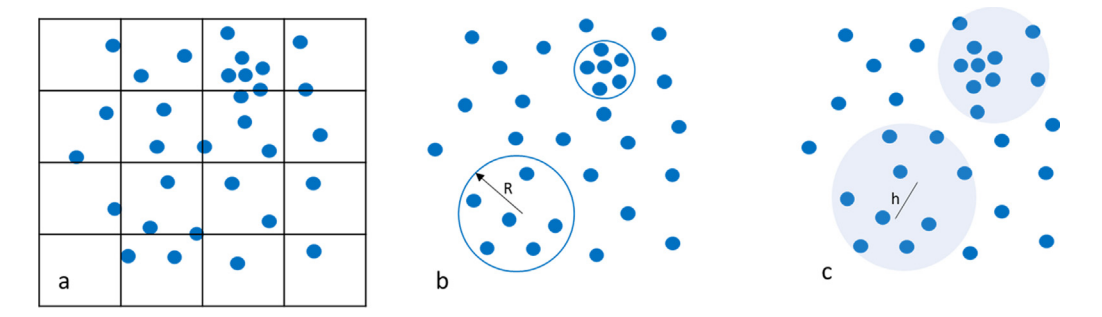
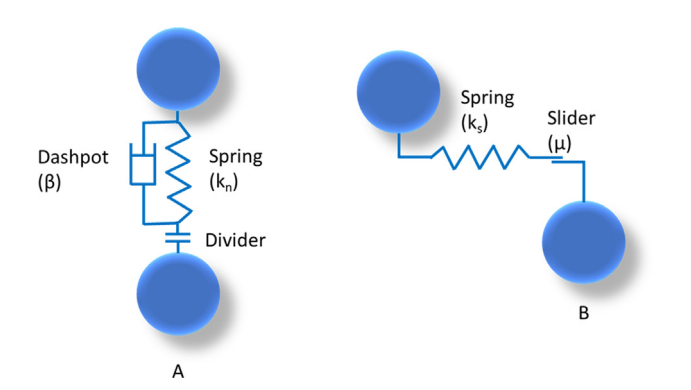


Fig. 11. Computing a continuous density field from a collection of point mass particles. Redrawn in agreement to the schematic in (Price 2012).



**Fig. 12.** The DEM contact model between two contacting particles. (A) Normal contact model, (B) Tangential contact model. Redrawn in agreement to the schematic in (Steinkogler et al., 2015).

terized by different volumetric responses. On the microscopic scale, detailed mechanisms of volumetric collapse were studied. Recently, the snow model was developed and calibrated based on the open source DEM code (Theile et al., 2020). In this model snow particles were characterized by randomly distributed elastic spheres connected by elastic-brittle bonds. This bonded structure relates to sintered snow. When external forces are applied, the stress in the bonds exceeds their strength, the bonds break, and loose particles, equivalent to granular snow, are formed. Model parameters are classified as temperature dependent material parameters and snow type dependent microstructure parameters. The model successfully reproduces the experimental results. (Theile et al., 2020). A new approach for FEM-DEM model was developed (Xu et al., 2020) in which the FEM of off-road tire was validated by stiffness tests, while the DEM of gravel particles was validated by triaxial compression tests. The calibrated FEM-DEM model can represent the off-road tire structural mechanics as well as the macroscopic mechanical characteristics of the gravel road.

Finally, the commercial software's like LS-DYNA was used to simulate the tractive performance of an off-road tire on a gravel road under varied slip conditions.

# 4. Conclusion

In the context of tire-terrain interaction simulations, the accuracy of the numerical model of the terrain is an important factor, especially when the terrain is compacted snow, which has received less attention. Improvements in snow models are still feasible due to either the inherent assumptions of a given modeling technique, the unpredictability of available snow data, and/or the poor inclusion of external influences on the sintering process of snow. The (semi) analytical methods requires important snow characteristics, such as mechanical properties and coefficient of friction between tire and the snow. However, due to lack of snow data, the analytical methods depend on various assumptions about snow mechanics. ALE based finite element technique to modeling snow has been employed and has been found to be successful. However, meshbased approaches suffer from substantial mesh distortion when dealing with large and discontinuous deformation and free surface flow. To overcome these problems, the DEM and SPH techniques have been started to be applied recently. These techniques are relatively new, and some improvements are still possible, particularly in terms computational expense. Overall, to better understand the advantages and disadvantages of the proposed numerical models, it would be useful to employ them in modeling the same tiresnow problem and evaluate their predictions (e.g. traction force) to corresponding test data.

# **Declaration of Competing Interest**

The authors declare that they have no known competing financial interests or personal relationships that could have appeared to influence the work reported in this paper.

## Acknowledgments

This study has been partially supported by the Center for Tire Research (CenTiRe), an NSF-I/UCRC (Industry/University Cooperative Research Center) at Virginia Tech, by the Terramechanics, Multibody and Vehicle Systems Laboratory (TMVS), and by the Center for Injury Biomechanics (CIB) at Virginia Tech. The authors wish to thank the project mentors and the members of the industrial advisory board of CenTiRe for their support and guidance.

#### References

- Abaqus, 2006. ABAQUS 6.6 Theory Manual. ABAQUS Inc..
- ABAQUS (2003). User's manual (Version 6.4).
- Abele, G., 1990. Snow road and runways. USA Cold Regions Research and Engineering Laboratory, Monograph (90-3).
- Abele, G., Gow, A.J., 1976. Compressibility Characteristics of Compacted Snow. Bader, H., 1963. Theory of densification of dry snow on high polar glaciers, 11, 351-376
- Addis, M.A. et al., 1993. The role of the intermediate principal stress in wellbore stability studies: evidence from hollow cylinder tests. Int. J. Rock Mech. Min. Sci. Geomech. Abstr. 30, 1027-1030.
- Bakker, E., Pacejka, H.B., Lidner, L., 1989. A New Tire Model with an Application in Vehicle Dynamics Studies. SAE International.

  Bažant, Z. P. (1985). "Mechanics of Geomaterials, Rocks, Concrete, Soils,".
- Bekker, M.G., 1969. Introduction to terrain-vehicle systems. University of Michigan Press, Ann Arbor.
- Borja, R., 1991. Cam-Clay plasticity, Part II: Implicit integration of constitutive equation based on a nonlinear elastic stress predictor. Comput. Methods Appl. Mech. Eng. 88, 225-240.
- Borja, R., Lee, S., 1990. Cam-clay plasticity, Part 1: Implicit integration of elastoplastic constitutive relations. Comput. Methods Appl. Mech. Eng. 78, 49-72.
- Browne, A., 1974. The physics of tire traction. Plenum Press.
- Bui, H., Sako, K., Fukagawa, R., 2007. Numerical simulation of soil-water interaction using smoothed particle hydrodynamics (SPH) method. J. Terramech. 44, 339-346
- Bui, H., Fukagawa, R., Sako, K., Ohno, S., 2008. Lagrangian mesh-free particle method (SPH) for large deformation and post-failure of geomaterial using elastic-plastic soil constitutive model. Int. J. Numer. Anal. Meth. Geomech. 32, 1537-1570.
- Bui, H., Nguyen, G., 2021. Smoothed particle hydrodynamics (SPH) and its applications in geomechanics: From solid fracture to granular behaviour and multiphase flows in porous media. Comput. Geotech. 138.
- Callari, C., Auricchio, F., Sacco, E., 1998. A finite-strain cam-clay model in the framework of multiplicative elasto-plasticity. Int. J. Plast. 14 (12), 1155-1187.
- Camponovo, C, Schweizer, J, 2001. Rheological measurements of the viscoelastic properties of snow. Annals of Glaciology 32, 44-50. https://doi.org/10.3189/ 172756401781819148.
- Carbone, A., Chiaia, B., Frigo, B., Türk, C., 2010. Snow metamorphism: a fractal approach. Phys. Rev. E: Stat. Nonlinear Soft Matter Phys. 82, 036103.
- Chang, C., Haimson, B., 2000. True triaxial strength and deformability of the German Continental Deep Drilling Program (KTB) deep hole amphibolite. J. Geophys. Res. Solid Earth 105 (B8), 18999-19013.
- Chen, W F, Mizuno, E, 1990. Nonlinear Analysis in Soil Mechanics: Theory and Implementation. Elsevier Science.
- Chiaia, B, Frigo, B, 2009. A scale-invariant model for snow slab avalanches. Journal of Statistical Mechanics: Theory and Experiment, P02056. https://doi.org/ 10.1088/1742-5468/2009/02/P02056.
- Choi, J.H., Cho, J.R., Woo, J.S., Kim, K.W., 2012. Numerical investigation of snow traction characteristics of 3-D patterned tire. J. Terramech. 49 (2), 81-93.
- Zienkiewicz, Olek C, Taylor, Zhu, J., 2005. The Finite Element Method: Its Basis and Fundamentals.
- Cresseri, S., Jommi, C., 2005. Snow as an elastic viscoplastic bonded continuum: a modelling approach. Italian Geotechnical J 4, 43-58.
- Cresseri, S., Genna, F., Jommi, C., 2010. Numerical integration of an elasticviscoplastic constitutive model for dry metamorphosed snow. Int. J. Numer. Anal. Meth. Geomech. 34, 1271-1296.
- Cundall, P.A., Strack, O.D.L., 1979. A discrete numerical model for granular assemblies. Geotechnique 29, 47-65.
- Desrues, J., Darve, F., Flavigny, E., Navarre, J.P., Taillefer, A., 1980. An incremental formulation of constitutive equations for deposited snow. J. Glaciol. 25 (92),
- Drucker, D.C., Prager, W., 1952. Soil mechanics and plastic analysis or limit design. Q. Appl. Math. 10 (2), 157-165.
- MSC.Dytran, 2002. User's Manual MSC.Software Corporation.
- El-Sayegh, Z., El-Gindy, M., 2018. Modelling and prediction of tyre-snow interaction using finite element analysis-smoothed particle hydrodynamics techniques. Proc. Inst. o Mech. Eng., D: J. Automob. Eng. 233 (7), 1783–1792.
- Fukue, M., 1979. Mechanical Performance of Snow Under Loading.
- Gaume J.C.G., Eckert, N., Naaim, M., 2012. Relative influence of mechanical and meteorological factors on ava lanche release depth distributions. Geophys. Res. Lett. 39(12), L12401.

- Gaume, J et al., 2011. Influence of weak layer heterogeneity on slab avalanche release using a finite element method. Adv. Bifurcation Degrad. Geomater., 23-
- Gaume, J et al., 2013. Influence of weak-layer heterogeneity on snow slab avalanche release: application to the evaluation of avalanche release depths. Journal of Glaciology 59 (215), 423-427. https://doi.org/10.3189/2013JoG12J161.
- Gheshlaghi, F., El-Sayegh, Z., El-Gindy, M., Oijer, F., Johansson, I., 2021. Advanced Analytical Truck Tires-Terrain Interaction Model. SAE International.
- Gheshlaghi, F., Mardani, A., mohebi, A., 2020. Investigating the effects of off-road vehicles on soil compaction using FEA-SPH simulation. Int. J. Heavy Vehicle Syst. 1.
- Gingold, R.A., Monaghan, J.J., 1977. Smoothed particle hydrodynamics: theory and application to non-spherical stars. MNRAS 181 (3), 375-389.
- Habermann, M., Schweizer, J., Jamieson, J.B., 2008. Influence of snowpack layering on human-triggered snow slab avalanche release. Cold Reg. Sci. Technol. 54 (3), 176-182.
- Haehnel, R., Shoop, S., 2004. A macroscale model for low density snow subjected to rapid loading. Cold Reg. Sci. Technol. 40, 193-211.
- Hambleton, J.P., Drescher, A., 2008. Modeling wheel-induced rutting in soils: Indentation. J. Terramech. 45 (6), 201-211.
- Hambleton, J.P., Drescher, A., 2009. Modeling wheel-induced rutting in soils: rolling. J. Terramech. 46 (2), 35-47.
- Han, L., Elliott, J., Bentham, A.C., 2008. A modified Drucker-Prager Cap model for die compaction simulation of pharmaceutical powders. Int. J. Solids Struct. 45, 3088-3106.
- Hashash, Y.M.A., Whittle, A.J., 1992. Integration of the modified Cam-Clay model in non-linear finite element analysis. Comput. Geotech. 14 (2), 59-83.
- Heierli, J., Zaiser, P.G.M., 2008. Anticrack nucleation as triggering mechanism for snow slab avalanches 321(5886), 240-243.
- HKS (Hibbitt, Karlsson, and Sorensen, Inc.), alysis of geotechnical problems with ABAQUS. Analysis of geotechnical problems with ABAQUS. ABAQUS Course Notes, Pawtucket, Rhode Island https://hungkcct.files.wordpress.com/2011/ 05/analysis-of-geotechnical-problems-with-abaqus.pdf,
- Janowski, W.R., 1980. Tire Traction Testing in the Winter Environment, SAE International.
- Jiang, H., 2011. A note on the Mohr-Coulomb and Drucker-Prager strength criteria. Mech. Res. Commun. 38.
- Johnson, J.B., Hopkins, M.A., 2005. Identifying microstructural deformation mechanisms in snow using discrete-element modeling. J. Glaciol. 51 (174), 432-442
- Kabore, B., Peters, B., Michael, M., Nicot, F., 2021. A discrete element framework for modeling the mechanical behaviour of snow-Part I: Mechanical behaviour and numerical model. Granular Matter 23.
- Karajan, N., Wang, J., Han, Z., Teng, H., Wu, C., Hu, W., Guo, Y., Fraser, K., 2014, 13. LS-DYNA® Forum.
- Kinosita, S., 1967. Compression of Snow at Constant Speed.
- Köchle, B., Schneebeli, M., 2014. Three-dimensional microstructure and numerical calculation of elastic properties of alpine snow with a focus on weak layers. J. Glaciol. 60 (222), 705-713.
- Kusachov, A., Bruzelius, F., Hjort, M., Jacobson, B.J.H., 2019. A double interaction brush model for snow conditions. Tire Sci. Technol. 47 (2), 118-140.
- Labuz, J.F., Zang, A., 2012. Mohr-Coulomb failure criterion. Rock Mech Rock Eng 2012 (45), 975-979.
- Lee, J.H., 2009. A new indentation model for snow. J. Terramech. 46 (1), 1–13.
- Lee, J., 2011a. Finite element modeling of interfacial forces and contact stresses of pneumatic tire on fresh snow for combined longitudinal and lateral slips. I. Terramech. 48, 171–197.
- Lee, J., 2011b. An improved slip-based model for tire-snow interaction. SAE Int. J. Mater. Manufact. 4, 278-288.
- Lee, J., 2013. Calibration and validation of a tire-snow interaction model. J. Terramech. 50, 289–302.
- Lee, J., 2016. Calibration of a simple cone-penetration model for snow. J. Terramech. 64. 36-45.
- Lee, J., Liu, Q., 2006. Interfacial Forces Between Tire and Snow Under Different Snow Depths.
- Lee, J., Liu, Q., Zhang, T., 2005. Predictive Semi-Analytical Model for Tire-Snow Interaction, SAE Technical Papers.
- Lee, J.H., Johnson, T.H., Huang, D., Meurer, S., Reid, A.A., Meldrum, B.R., 2010. New integrated testing system for the validation of vehicle-snow interaction models. ALASKA UNIV FAIRBANKS.
- LeVeque, R.J., 2002. Finite Volume Methods for Hyperbolic Problems. Cambridge, Cambridge University Press.
- Lever, J.H., Denton, D., Phetteplace, G., Wood, S.D., Shoop, S.A., 2006. Mobility of a lightweight tracked robot over deep snow. J. Terramech. 43, 527-551.
- Lucy, L.B., 1977. A numerical approach to the testing of the fission hypothesis. The Astron. J. 82, 1013-1024.
- Lundy, Chris C. et al., 2002. Measurement of snow density and microstructure using computed tomography. Journal of Glaciology 48 (161), 312-316. https://doi. org/10.3189/172756502781831485. Mellor, M., 1975. A review of basic snow mechanics. IASH pub 114, 251–291.
- Mellor, M., 1977. Engineering properties of snow. J. Glaciol. 19 (81), 15-66.
- Meschke, G., 1995. New viscoplastic model for snow at finite strains. Proc Int. Conf. Computat. Plast., 2295-2306
- Meschke, G., Liu, C., Mang, H., 1996. Large strain finite-element analysis of snow. J. Eng. Mech.-Asce - J ENG MECH-ASCE 122.

- Moos, M. v., P. Bartelt, A. Zweidler, Bleiker, E., 2003. Triaxial tests on snow at low strain rate. Part I. Experimental device. J. Glaciol. 49(164), 81–90.
- Moukalled F.M.L., Darwish, M., 2016. The Finite Volume Method in Computational Fluid Dynamics.
- Mulak, D., Gaume, J., 2019. Numerical investigation of the mixed-mode failure of snow. Computat. Part. Mech. 6 (3), 439–447.
- Mundl, R., Meschke, G., Liederer, W., 1997. Friction mechanism of tread blocks on snow surfaces. Tire Sci. Technol. 25, 245–264.
- Muro, T., Yong, R., 1980. Rectangular plate loading test on snow. J. the Japanese Soc. Snow and Ice 42, 17–24.
- Nadai, A., 1950. Theory of flow and fracture of solids. McGrawHill, New York.
- Nakajima, Y., 2003. Analytical model of longitudinal tire traction in snow. J. Terramechanics J TERRAMECH 40, 63–82.
- Narita, H., 1984. An experimental study on tensile fracture of snow. Contribut. Inst. Low Temp. Sci. 32, 1–37.
- Nova, R., 1992. Mathematical modelling of natural and engineering geomaterials. Eur. J. Mech., A/ Solids 11, 35–154.
- Oida, S., Seta, E., Heguri, H., Kato, K., 2005. Soil/tire interaction analysis using FEM and FVM. Tire Sci. Technol. 33 (1), 38–62.
- Peinke, I., Hagenmuller, P., Andò, E., Chambon, G., Flin, F., Roulle, J., 2020. Experimental study of cone penetration in snow using X-Ray tomography. Front. Earth Sci. 8.
- Peters, B., Kabore, B.W., Michael, M., Nicot, F., 2021. A discrete element framework for modeling the mechanical behaviour of snow Part II: model validation. Granular Matter 23 (2), 43.
- Podolskiy, E., Chambon, G., Naaim, M., Gaume, J., 2013. A review of finite-element modelling in snow mechanics. J. Glaciol. 59, 1189–1201.
- Potts, D., Zdravkovic, L., 1999. Some Pitfalls when using Modified Cam Clay.
- Podolskiy, E. 2014. Healing of snow surface-to-surface contacts by isothermal sintering. The Cryosphere 8, 1651–1659. https://doi.org/10.5194/tc-8-1651-2014.
- Price, D.J., 2012. Smoothed particle hydrodynamics and magnetohydrodynamics. J. Comput. Phys. 231 (3), 759–794.
- Rao, S.S., 2017. The finite element method in engineering.
- Reuter, B., Proksch, M., LÖWe, H., Van Herwijnen A., Schweizer, J., 2019. Comparing measurements of snow mechanical properties relevant for slab avalanche release. J. Glaciol. 65(249), 55-67.
- Rooney, T., Satrape, J., Liu, S., 2002. Application of finite element analysis and computational fluid dynamics to ATV tire design. Tire Sci. Technol. 30 (3), 198–212.
- Roscoe, K.H.a.B., J.B., 1968. On the generalized stress-strain behaviour of 'wet clay' Engineering plasticity. Cambridge University Press.: 535–609.
- Rocscience, eory Manuals: Cam Clay and Modified Cam Clay Material Models.
  Theory Manuals: Cam Clay and Modified Cam Clay Material Models https://www.rocscience.com/help/rsdata/verification-theory/theory-manuals.
- Salm, B., 1982. Mechanical properties of snow. Rev. Geophys. Space Physics 20, 1-
- Sanderson, T, 1988. Ice Mechanics Risks to Offshore Structures. Publ. Graham and Trotman, Landon.
- Sandler et al., 2002. Review of the development of cap models for geomaterials. 15th ASCE Engineering Mechanics Conference, Columbia University, New York.
- Scapozza, C., 2004. Entwicklung eines dichte und temperaturabhängigen Stoffgesetzes zur Beschreibung des visko-elastischen Verhaltens von Schnee PhD Thessis, ETH Zürich.
- Scapozza, C., Bartelt, P., 2003a. Triaxial tests on snow at low strain rate. Part II. Constitutive behaviour. J. Glaciol. 49 (164), 91–101.
- Scapozza, C., Bartelt, P.A., 2003b. The influence of temperature on the small-strain viscous deformation mechanics of snow: a comparison with polycrystalline ice. Ann. Glaciol. 37, 90–96.

- Schneebeli, M., Pielmeier, C., Johnson, J.B., 1999. Measuring snow microstructure and hardness using a high resolution penetrometer. Cold Reg. Sci. Technol. 30 (1), 101–114.
- Schulson, E.M., Duval, P., 2009. Creep and fracture of ice. Cambridge University
- Schweizer, J. et al., 2003. Snow avalanche formation. Reviews of Geophysics 41 (4). https://doi.org/10.1029/2002RG000123.
- Schweizer, J. 2011. Measurements of weak layer fracture energy. Cold Reg. Sci. Tech 69 (2–3), 139–144. https://doi.org/10.1016/j.coldregions.2011.06.004.
- Seta, E., Kamegawa, T., Nakajima, Y., 2003. Prediction of snow/tire interaction using explicit FEM and FVM. Tire Sci. Technol. 31 (3), 173–188.
- Seta, E., Nakai, T., Heggli, M., Jaggi, M., Löwe, H., Schneebeli, M., Szabo, D., 2010.

  Prediction of tire traction on a compacted snow road. Phys. Chem. Ice 2010, 45–49
- Shapiro, L., Johnson, J., Sturm, M., Blaisdell, G., 1997. Snow Mechanics: Review of the State of Knowledge and Applications 40.
- Shenvi, M., Sandu, C., Untaroiu, C., 2022. Review of compressed snow mechanics: testing methods. J. Terramech. 100, 25–37.
- Shoop, S., Phetteplace, G., Wieder, W., 2010. Snow Roads at McMurdo Station, Antarctica.".
- Shoop, S.A., 2001. Finite Element Modelling of Tire-Terrain Interaction.
- Sigrist, C., 2006. Measurement of fracture mechanical properties of snow and application to dry snow slab avalanche release.
- Simo, J.C., Meschke, G., 1993. A new class of algorithms for classical plasticity extended to finite strains. application to geomaterials. Comput. Mech. 11 (4), 253–278
- Smith, F.W., 1972. Elastic stresses in layered snow packs. J. Glaciol.
- Smith, F.W., S.R.a. B R., 1971. Finite-element stress analysis of avalanche snowpacks. J. Glaciol. 10(60), 401–405.
- Srivastava, P.K., Chandel, C., Mahajan, P., Pankaj, P., 2016. Prediction of anisotropic elastic properties of snow from its microstructure. Cold Reg. Sci. Technol. 125, 85–100
- Steinkogler, W., Gaume, J., Löwe, H., Sovilla, B., Lehning, M., 2015. Granulation of snow: From tumbler experiments to discrete element simulations. J. Geophys. Res.: Solid Earth 120.
- Svendenius, J., 2003. Tire Models for Use in Braking Applications.
- Terziyski, J., 2010. Tire performance evaluation for severe snow traction. 2010 SIMULIA Customer Conference.
- Theile, T., Szabó, D., Willibald, C., Schneebeli, M., 2020. Discrete element model for high strain rate deformations of snow. <u>arXiv: Geophysics</u>.
- Van Herwijnen, A., Gaume, J., Bair, E.H., Reuter, B., Birkeland, K.W., Schweizer, J., 2016. Estimating the effective elastic modulus and specific fracture energy of snowpack layers from field experiments. J. Glaciol. 62 (236), 997–1007.
- Voitkovsky, K.F., Bozhinsky, A.N., Golu bev, V.N., Laptev, M.N., Zhigulsky, A.A., Yu Ye, Slesarenko, 1975. Creep induced changes in structure and density of snow. Int. Sympos. Snow Mech., Grindelwald, Switzerland 114, 171–179.
- Wang, E., Fu, X., Han, H., Liu, X., Xiao, Y., Leng, Y., 2021. Study on the mechanical properties of compacted snow under uniaxial compression and analysis of influencing factors. Cold Reg. Sci. Technol. 182, 103215.
- Wautier, A., Geindreau, C., Flin, F., 2015. Linking snow microstructure to its macroscopic elastic stiffness tensor: a numerical homogenization method and its application to 3-D images from X-ray tomography. Geophys. Res. Lett. 42 (19), 8031–8041.
- Wong, J.Y., 1993. Theory of ground vehicles. J. Wiley, New York, N.Y.
- Xu, W., Zeng, H., Yang, P., Zang, M., 2020. Numerical analysis on tractive performance of off-road tire on gravel road using a calibrated finite element method-discrete element method model and experimental validation. In: Proceedings of the Institution of Mechanical Engineers, Part D: Journal of Automobile Engineering 234: 095440702093017.
- Yu, M.-H., 2002. Advances in strength theories for materials under complex stress state in the 20th Century. Appl. Mech. Rev. 55, 169–218.